
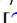

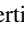


Mean path length inside nonscattering refractive objects

Matt Majic ^{*}, Walter R. C. Somerville [†], and Eric C. Le Ru [‡]

The MacDiarmid Institute for Advanced Materials and Nanotechnology, School of Chemical and Physical Sciences, Victoria University of Wellington, P.O. Box 600 Wellington, New Zealand

 (Received 26 August 2020; accepted 1 March 2021; published 16 March 2021)

It was recently argued that the geometric optics mean path length of rays inside a refractive object under Lambertian illumination is independent of the scattering strength of the medium [Savo *et al.*, *Science* **358**, 765 (2017)]. We here show that it is, in fact, different in the case of zero scattering. We uncover and explain the role of trapped ray trajectories in creating this unexpected discontinuity from zero to low scattering. This allows us to derive alternative analytic results for the zero scattering mean path length of simple refractive shapes. We believe this work provides a fresh perspective on the study of path length inside refractive objects, with possible applications in, for example, the study of scattering by large particles or the design of optical systems.

DOI: [10.1103/PhysRevA.103.L031502](https://doi.org/10.1103/PhysRevA.103.L031502)

Finding the mean chord length for a random distribution of lines in a given object is a natural question in many areas of physics. It is a seemingly complex task from a mathematical perspective since one should consider the spatial and angular distribution of lines as well as how they intersect the surface of the object. For convex bodies the answer is, however, surprisingly simple, given by the mean chord length theorem, which has been known for more than a century [1]. It states that the mean chord length (C) is independent of the shape of the object and depends on only the ratio of volume V to surface area Σ as $\langle C \rangle = 4V/\Sigma$. Proofs from various perspectives have been given [2–4]. It was only fairly recently shown that this theorem can be generalized further to the study of random walks in diffusive objects. The mean *path* length theorem [5] states that the mean path length is still simply $\langle L \rangle = 4V/\Sigma$; this is independent of both shape and the scattering/diffusive properties of the medium. The validity extends across many fields as it is valid for any random walk inside an object and is particularly relevant to geometric optics within a closed scattering medium. One important condition for this theorem is that the entrance point and initial direction are uniformly and isotropically distributed, which in optics is equivalent to a Lambertian illumination [2].

Path length distributions and mean path length are central to the design of many optical systems where a ray optics description can be used. They can be used for calculating the optical properties of absorbing and scattering media [6,7], refractive granular media in pharmaceutical powders [8], for solar cell design [9–11], random lasing [12], and integrating spheres [13,14]. Ray tracing can also be combined with diffraction effects to calculate the electromagnetic scattering properties of large particles in models such as the geometric optics approximation and physical optics model [15–20] or

anomalous diffraction theory [21–23]. These models have, for example, been applied to the study of ice crystals [17,18,20] for climate modeling. The zero scattering mean path length is directly related to the orientation-averaged absorption cross sections of large absorbing particles [24–26]. Path length distributions have also been used to derive the scattering phase function of an object analytically [27].

In most of these applications, the object has a different refractive index than the surrounding medium. Rays are then refracted at the boundary and may also be reflected internally or externally, which may increase the path length of some internal rays. Even then, it was argued recently [28,29] that the mean path length invariance remains valid for scattering samples and is simply modified by a factor s^2 :

$$\langle L \rangle = \frac{4V}{\Sigma} s^2 \quad (1)$$

for any three-dimensional (3D) convex body, independent of the scattering properties of the sample. A justification of Eq. (1) was given assuming a thermodynamic equilibrium and equipartition [28,29] and following energy conservation arguments drawing on the discussion in Ref. [30]. In this Letter, we focus on the mean path length in the low-scattering limit. The equipartition assumption and Eq. (1) also apply, but we will show that the zero scattering case is different, resulting in a discontinuous transition between low and zero scattering for some geometries. This result is related to the existence of trapped paths (similar to the whispering gallery trajectories inside a sphere), which cannot be populated in the strict absence of scattering. To further support this argument, we have derived a number of analytic expressions for the zero scattering mean path length inside simple two-dimensional (2D) and 3D refractive objects. They demonstrate the discontinuity at zero scattering, and their derivations support the physical interpretations in terms of trapped rays. Less symmetric geometries are also studied using Monte Carlo ray-tracing simulations [29], allowing us to discuss the generality

^{*}mattmajic@gmail.com

[†]walter.somerville@vuw.ac.nz

[‡]eric.leru@vuw.ac.nz

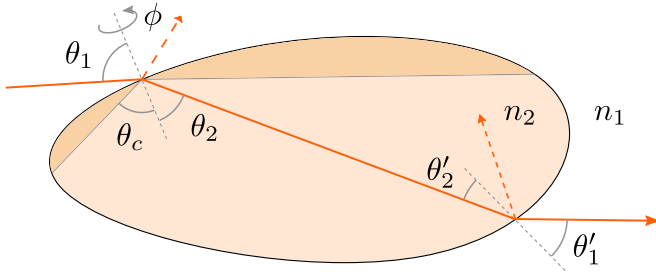


FIG. 1. A light ray being refracted as it passes from medium 1 to medium 2. The darker region in medium 2 is not accessible from rays entering from medium 1.

of this discontinuity, its sensitivity to imperfections, and its relevance to applications.

Mean path length in a refractive sample. We consider, as shown in Fig. 1, a nonabsorbing convex body V_2 embedded in an outside medium V_1 with refractive indices $n_2 > n_1$ and define $s = n_2/n_1 > 1$. At this stage, we do not exclude the possibility that medium 2 is a scattering medium. We study the trajectory of light rays within the geometric optics approximation, as they undergo stochastic refraction or reflection at the interface. Consider a ray incident on the surface, with an angle of incidence θ_1 to the surface normal, and rotated by ϕ around it. The ray may be refracted at an angle θ_2 with a probability $T_{12}(\theta_1)$ with $\sin \theta_1 = s \sin \theta_2$ (Snell's law), while the azimuthal angle ϕ is unaffected. By optical reciprocity, the probabilities of transmission at complementary angles are identical: $T_{12}(\theta_1) = T_{21}(\theta_2)$. Similar laws apply to internal rays hitting the object surface with internal θ'_2 and external θ'_1 angles. Since $n_2 > n_1$, angles θ'_2 above the critical angle $\theta_c = \text{asin}(1/s)$ have zero transmission: there is total internal reflection (TIR).

As for the mean path (or chord) length theorems, we assume that the illumination of the object from the outside is Lambertian. The surface irradiance is therefore uniform, and the incident angles follow the probability distribution $p(\theta_1) = 2 \cos \theta_1 \sin \theta_1 = \sin(2\theta_1)$ ($0 \leq \theta_1 < \pi/2$) in three dimensions [2]. Because Lambertian illumination maximizes entropy and energy is conserved in the scattering process, the ensemble of external rays reflecting and internal rays exiting must also follow a Lambertian distribution (otherwise, entropy would have been decreased). Then, since incident and outgoing rays have the same distribution, for every internal ray making an angle $\theta'_2 < \theta_c$ to the normal [and reflected with a probability $p_2 = 1 - T_{21}(\theta'_2)$], there is an incident external ray that is externally reflected at the Snell-matching θ'_1 with the same probability $p_1 = 1 - T_{12}(\theta'_1) = p_2$; that is, there is a one-to-one correspondence between these rays (see Sec. S.I in the Supplemental Material [31] for more detail). This allows us to ignore all internally reflected rays with $\theta'_2 < \theta_c$ in mean path length calculations if we also ignore any reflection from the outside (dashed rays in Fig. 1). These externally reflected rays would normally have zero path length, but if they were to transmit inwards, they would have exactly the path length and angular distribution of the rays that reflect from the inside for $\theta'_2 < \theta_c$. See also Sec. S.II for an explicit example of this cancellation in simple geometries. This is a crucial

feature for refractive objects, as it simplifies the calculations dramatically. Note, however, that the contribution of rays with $\theta'_2 > \theta_c$ (TIRs), whose distribution is not specified, must still be accounted for.

This result also highlights that Eq. (1) for scattering media assumes that these externally reflected rays with $L = 0$ are included in the statistics, an important point that was not made explicit in Refs. [28,29]. The mean path length not counting $L = 0$ rays can be simply deduced as $\langle L_{L>0} \rangle = \langle L \rangle / \bar{T}_{12}$, where \bar{T}_{12} is the Lambertian-averaged transmission [32].

Following these considerations, we may express the mean path length in the object as

$$\langle L \rangle = \int_{\Sigma} \frac{d\Sigma}{\Sigma} \int \frac{d\phi}{2\pi} \int_0^{\pi/2} d\theta_1 L(\mathbf{r}, \theta_1, \phi) \sin(2\theta_1), \quad (2)$$

where $L(\mathbf{r}, \theta_1, \phi)$ denotes the total ray path length for a given entry point \mathbf{r} and incidence angles, including possible total internal reflections until it reaches the surface with $\theta'_2 < \theta_c$ (thanks to the cancellation between internal and external reflections). In the absence of scattering and total internal reflections, L then coincides with the chord length C . In the presence of scattering L should be understood as an average over all possible scattering paths, which renders this ray approach difficult.

We have applied this method to several standard geometries in the nonscattering case and obtained analytical results for simple shapes and numerical results for more complex shapes. The most surprising outcome is that the zero scattering mean path length $\langle L^0 \rangle$ is different (smaller) from the scattering mean path length $\langle L \rangle$ for some geometries, which results in a discontinuous transition at zero scattering. We first discuss further this counterintuitive result as it will provide physical insight into its origin and provide an alternative method of calculating $\langle L^0 \rangle$ in special cases.

Transition between the low- and zero-scattering regimes. To understand how this discontinuous transition arises, we will attempt to connect the two different approaches for the scattering (thermodynamic) and nonscattering (ray optics) cases. Specifically, we here derive the mean path length $\langle L \rangle$ in the low-scattering limit from $\langle L^0 \rangle$ using a ray-optics argument. At the center of this discussion is the existence of trapped rays. These undergo successive TIRs and cannot escape, similar to propagating modes in an optical fiber or whispering gallery modes in dielectric spheres. Note that these trajectories may be repeating (as the optical modes) or chaotic. Because of reciprocity, these rays cannot be excited from outside in the ray optics framework and therefore are irrelevant to $\langle L^0 \rangle$.¹ But if scattering is present, then there is a probability that some rays are scattered into and out of trapped trajectories. For very low scattering, this probability is small, and one might expect that it does not affect the mean path length. However, trapped

¹Note that arbitrarily long path lengths may still exist, for example, in the 2D ellipse, where rays that refract in at almost the critical angle at the tips will undergo a large number of total internal reflections before inevitably refracting out. In terms of the elliptical billiard table [33], the rays would enter at a trough on the phase portrait that touches the line at the critical angle. However, these are not strictly trapped.

rays exhibit very long path lengths because scattering is low. It is this product of a small probability by a large path length that may result in a finite, nonzero contribution to $\langle L \rangle$ even in the limit of zero scattering but not for zero scattering, hence the discontinuity.

To be more quantitative, we denote the scattering coefficient α and assume that the scattering mean free path $l_\alpha = 1/\alpha$ is much greater than $\langle L^0 \rangle$. For simplicity, we will here consider special cases where the probability of scattering into a trapped trajectory, denoted P_T , is independent of the position of the scattering event. A more general case is discussed in Sec. S.III. The average probability of a ray scattering is $\alpha \langle L^0 \rangle \ll 1$. Since the average path length for nontrapped rays is of order $\langle L^0 \rangle$, scattering into them results in negligible changes to path length (of order $\alpha \langle L^0 \rangle^2$). In contrast, a ray will escape a trapped path only if it is scattered again, which results in an average path length $l_\alpha \gg \langle L^0 \rangle$ for trapped rays. Moreover, scattering may occur into another trapped path with probability P_T , which increases the path length by l_α again until the next scattering event. Summing, we obtain the mean path length for trapped rays as

$$\langle L^T \rangle = l_\alpha + P_T l_\alpha + P_T^2 l_\alpha + \dots = \frac{l_\alpha}{1 - P_T}. \quad (3)$$

$\langle L^T \rangle \gg \langle L^0 \rangle$, but this is compensated by the small probability $\alpha \langle L^0 \rangle P_T$ of scattering into a trapped trajectory. We can now add this contribution to $\langle L^0 \rangle$ to obtain the low-scattering mean path length:

$$\langle L \rangle \approx \langle L^0 \rangle + [\alpha \langle L^0 \rangle P_T] \langle L^T \rangle = \frac{\langle L^0 \rangle}{1 - P_T}. \quad (4)$$

This derivation provides an explanation for the discontinuity at zero scattering, which is due to the second term, related to trapped trajectories. Equation (4), moreover, provides a simple method of deducing $\langle L^0 \rangle$ analytically for objects where P_T is independent of position and angle, which includes many objects with faceted sides. An important special case is for objects where no trapped rays can be supported ($P_T = 0$), for which $\langle L^0 \rangle = \langle L \rangle$. Among these are objects with a refractive index smaller than the embedding medium ($s < 1$). The consideration of trapped paths also suggests a link between this problem and the theory of “billiards” in classical mechanics [33]. In particular, ergodic shapes will also automatically have $P_T = 0$ (since every ray samples the entire phase space) and therefore $\langle L^0 \rangle = \langle L \rangle$.

Analytic results. To further illustrate this discussion, we now provide a collection of analytic results that we have derived for $\langle L^0 \rangle$ in simple 3D and 2D geometries. The main 3D geometries that we considered are summarized in Fig. 2, where their parameters are defined. The advantage of these ideal geometries is that the derivations illustrate how concepts such as trapped rays affect the mean path length. The derived $\langle L^0 \rangle$ as a function of s for all 3D geometries are summarized and compared to the scattering case in Fig. 3. To calculate $\langle L^0 \rangle$, we use Eq. (2), rewritten in terms of the inside angle as

$$\langle L^0 \rangle = s^2 \int_{\Sigma} \frac{d\Sigma}{\Sigma} \int \frac{d\phi}{2\pi} \int_0^{\theta_c} d\theta_2 L(\mathbf{r}, \theta_2, \phi) \sin(2\theta_2). \quad (5)$$

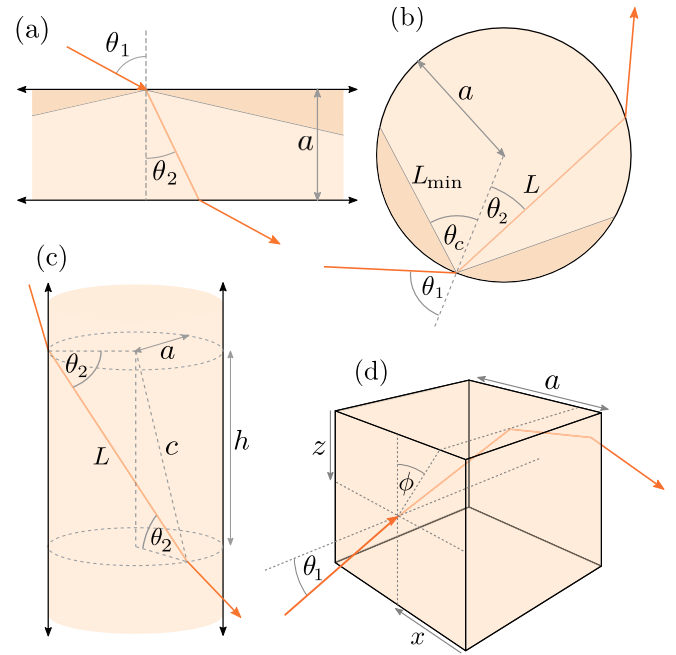


FIG. 2. Main geometries considered in this work: (a) the 2D strip and 3D slab, (b) the circle and sphere, (c) the infinite cylinder, and (d) the cube and cuboid. We also treat the square, rectangle, and infinite square rod.

We start with the simplest case of an infinite slab of width a [Fig. 2(a)]. In this case, $L(\mathbf{r}, \theta_2, \phi)$ depends on only θ_2 . Moreover, since we can ignore probabilistic reflections and it is not possible to excite TIRs from the outside, L is the same as the chord length, so we have $L = a / \cos \theta_2$, and the mean

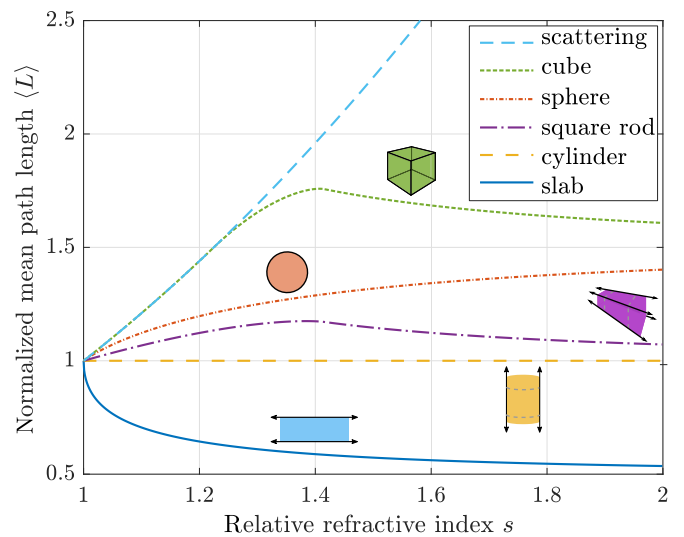


FIG. 3. Comparison of the s dependence of the zero-scattering mean path length $\langle L^0 \rangle$ for 3D objects for which analytical expressions were derived. All values are normalized to the mean chord length $\langle C \rangle = 4V/\Sigma$. The scattering case $\langle L \rangle = s^2 \langle C \rangle$ is shown as a dashed line.

is calculated as

$$\langle L_{\text{slab}}^0 \rangle = 2as^2(1 - \cos \theta_c) = 2as^2 \left(1 - \sqrt{1 - \frac{1}{s^2}} \right). \quad (6)$$

This could also have been deduced from Eq. (4) since the trapping probability is uniform: $P_T = \cos \theta_c$. $\langle L_{\text{slab}}^0 \rangle$ decreases with s (see Fig. 3) and is less than the mean path length for a slab with scattering, $\langle L_{\text{slab}} \rangle = 2as^2$.

For a sphere of radius a [Fig. 2(b)], $L(\mathbf{r}, \theta_2, \phi)$ again depends on only θ_2 , and it is not possible to excite TIRs from the outside, so we have $L = 2a \cos \theta_2$ (the chord length) and, integrating Eq. (5),

$$\langle L_{\text{sphere}}^0 \rangle = \frac{4a}{3}s^2 \left[1 - \left(1 - \frac{1}{s^2} \right)^{3/2} \right]. \quad (7)$$

This expression appears, for example, in the absorption cross section for large weakly absorbing spheres [19,25]. For comparison, the mean path length for a sphere with scattering is $\langle L_{\text{sphere}} \rangle = (4/3)as^2$. We cannot here use Eq. (4) because the probability of trapping P_T depends on position: trapping is more likely for scattering events close to the sphere surface.

For the cube [Fig. 2(d)], there are three regimes depending on s . First, we can show that for $s \leq \sqrt{3/2}$, no trapped rays exist; hence, $P_T = 0$, and

$$\langle L_{\text{cube}}^0(s \leq \sqrt{3/2}) \rangle = \langle L_{\text{cube}} \rangle = \frac{2}{3}as^2. \quad (8)$$

For $s \geq \sqrt{2}$, we may use Eq. (5); the problem is simplified by the fact that all rays exit the opposite face of the cube. Some will totally internally reflect on an adjacent face [see Fig. 2(d)], and some will exit straight through, but in both cases, the path length is given as $L = a / \cos \theta_2$; therefore, we obtain

$$\langle L_{\text{cube}}^0(s \geq \sqrt{2}) \rangle = 2as^2 \left(1 - \sqrt{1 - \frac{1}{s^2}} \right). \quad (9)$$

In the intermediate case, $\sqrt{3/2} < s < \sqrt{2}$, calculating $\langle L_{\text{cube}}^0 \rangle$ via Eq. (5) is rather technical (see Sec. S.IV). We present in Sec. S.V a simpler derivation using Eq. (4), which applies because the trapping probability P_T is again independent of the location of the scattering event. Both result in

$$\begin{aligned} \langle L_{\text{cube}}^0(\sqrt{3/2} < s < \sqrt{2}) \rangle &= \frac{4as^2}{\pi} \left(\sin^{-1}(s^2 - 1) - \sqrt{1 - \frac{1}{s^2}} \sin^{-1}(2s^2 - 3) \right). \end{aligned} \quad (10)$$

A similar derivation can be carried out for a cuboid with edges a, b, c , and the results are the same with the transformation:

$$a \rightarrow \frac{3abc}{ab + bc + ca}, \quad (11)$$

i.e., rescaled by the relative factor V/Σ for each shape. The cases of an infinite circular cylinder [Fig. 2(c)] and an infinite square rod are also derived and discussed in Secs. S.VI and S.VII.

Finally, 2D objects can be treated with a similar approach. We have obtained analytic expressions for $\langle L^0 \rangle$ for an infinite strip, a circle, a square, and a rectangle. The results and

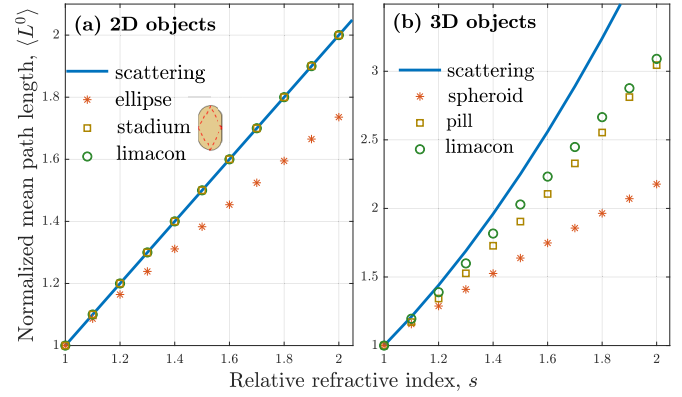


FIG. 4. Comparison of the s dependence of the zero-scattering mean path length $\langle L^0 \rangle$ for less symmetric objects. All values are normalized to the mean chord length $\langle L \rangle$, and the scattering case $\langle L \rangle$ is shown as a solid line. (a) Two-dimensional objects: ellipse and stadium of aspect ratio 2 and Pascal's limaçon of polar equation $r(\theta) = b + a \cos \theta$, with $b/a = 3$. (b) Three-dimensional objects: same as 2D objects with symmetry of revolution around z .

derivations are provided in Sec. S.VIII, along with a graphical summary. The conclusions are similar to those for 3D objects.

Application to physical systems. To investigate the generality of these results, we now consider less symmetric geometries, for which numerical calculations (Monte Carlo ray tracing [29]) can be used to derive $\langle L^0 \rangle$. Figure 4 summarizes these results. We consider explicitly in Fig. 4(a) 2D shapes with different refractive indices and decreasing symmetries: ellipse, stadium, and a convex limaçon. The latter two do not show any discontinuity within our numerical accuracy, i.e., $\langle L^0 \rangle = \langle L \rangle$, even at high refractive index, which suggests that the probability of scattering into a trapped trajectory is zero. Note that trapped rays may still exist [such as the one depicted for the stadium in Fig. 4(a)], but they correspond to unstable orbits with vanishingly small probabilities of being scattered into. The situation is different for ellipses where a larger number of rays may be trapped, in agreement with the theory of elliptical billiards [33]. Interestingly, corresponding 3D objects with symmetry of revolution all show $\langle L^0 \rangle < \langle L \rangle$, likely because of the trapped trajectories in the planes perpendicular to the revolution axis. It would be interesting to further link these results to the theory of classical billiards, chaos and ergodicity, but that is outside the scope of this Letter.

Figure 4 overall suggests that the mean path length discontinuity is a special property of geometries with higher symmetry. These special shapes are, nevertheless, commonly used as model systems in many applications. As an example, ice crystals are often taken as high-symmetry objects to derive their optical properties for atmospheric models [17,18,20]. Within the geometric optics approximation [17,19], the absorption cross section C_{abs} of weakly absorbing objects is directly proportional to the *zero-scattering* mean path length. The expressions we obtained (and more that could be derived using the same approach) can then be used to derive an analytic expression. For example, for a $5\text{-}\mu\text{m}$ -wide ice cube at $\lambda = 1\text{ }\mu\text{m}$ ($s = s' + is'' = 1.3 + 1.6 \times 10^{-6}i$), we find that

the analytic prediction

$$\begin{aligned} \langle C_{\text{abs}} \rangle &\approx \frac{4\pi s''}{\lambda} \langle L_{\text{cube}}^0(s') \rangle \\ &\approx \frac{16as'^2 s''}{\lambda} \left(\sin^{-1}(s'^2 - 1) - \sqrt{1 - \frac{1}{s'^2}} \sin^{-1}(2s'^2 - 3) \right) \end{aligned} \quad (12)$$

agrees within $\pm 10\%$ with numerical calculations. This approach is valid for particle sizes much larger than the wavelength but smaller than the characteristic absorption length, i.e., $1 \ll (2\pi/\lambda)a \lesssim (1/s'')$. Together with the approximate extinction cross section $\langle C_{\text{ext}} \rangle \approx 3a^2$, these provide simple analytical inputs for atmospheric models over a large size range, replacing the time-consuming ray tracing simulations otherwise required. This approach could be generalized to more realistic ice crystal shapes and to other weakly absorbing atmospheric aerosols.

Apart from such applications, while the zero scattering discontinuity is interesting from a fundamental point of view, we should also consider its relevance to real physical systems. First, all physical media are imperfect and should exhibit a small, but nonzero, scattering coefficient. Second, surface imperfections are unavoidable, be they roughness or a small deviation from ideal shapes (likely to make the object nonconvex). Third, the ray optics description is only an approximation, and wave effects can affect reflection and refraction, in particular resulting in a small probability of out-coupling during TIR events, which would preclude the

existence of strict trapped trajectories. Because of these effects, one could argue that the zero scattering discontinuity is irrelevant and the general formula [Eq. (1)] applies instead. However, one should also consider that any physical medium has a nonzero absorption coefficient. This small absorption negates the contribution of extremely long-lived trapped rays for low scattering, so that the relevant experimental mean path length is, in fact, the zero scattering one, as long as the scattering is smaller than the absorption coefficient. This argument is developed more qualitatively in Sec. S.IX.

Conclusion. We have examined how shape affects the mean path length of rays in nonscattering refractive objects, providing the theoretical groundwork to derive the mean path length analytically and applying it to simple shapes. Crucial to being able to derive these results was the fact that all probabilistic reflections below the critical angle can be discounted if they are ignored from both the inside and outside. We believe that some other geometries will be able to be treated using the same approach. These analytic results also highlight explicitly the discontinuous transition from nonscattering to scattering media and demonstrate that it is due to the existence of trapped trajectories that cannot be occupied without scattering.

We believe this work is an important contribution to the resurgent study of path length invariance in media. The derived analytic expressions will also be useful in other theoretical contexts where mean path length, or path length distributions, are studied, as refractive nonscattering objects are central to many applications.

Acknowledgment. The authors are grateful to the MacDiarmid Institute, New Zealand, for financial support.

-
- [1] E. Czuber, Zur theorie der geometrischen wahrscheinlichkeiten, *Sitzungsber. Akad. Wiss. Wien* **90**, 719 (1884).
- [2] A. M. Kellerer, Considerations on the random traversal of convex bodies and solutions for general cylinders, *Radiat. Res.* **47**, 359 (1971).
- [3] R. Coleman, Random paths through convex bodies, *J. Appl. Probab.* **6**, 430 (1969).
- [4] W. J. M. De Kruijf and J. L. Kloosterman, On the average chord length in reactor physics, *Ann. Nucl. Energy* **30**, 549 (2003).
- [5] S. Blanco and R. Fournier, An invariance property of diffusive random walks, *Europhys. Lett.* **61**, 168 (2003).
- [6] R. Mupparapu, K. Vynck, T. Svensson, M. Burrelli, and D. S. Wiersma, Path length enhancement in disordered media for increased absorption, *Opt. Express* **23**, A1472 (2015).
- [7] F. Tommasi, L. Fini, F. Martelli, and S. Cavalieri, Invariance property in scattering media and absorption, *Opt. Commun.* **458**, 124786 (2020).
- [8] O. Scheibelhofer, P. R. Wahl, B. Larchevêque, F. Chauchard, and J. G. Khinast, Spatially resolved spectral powder analysis: Experiments and modeling, *Appl. Spectrosc.* **72**, 521 (2018).
- [9] A. N. Sprafke and R. B. Wehrspohn, Current concepts for optical path enhancement in solar cells, in *Photon Management in Solar Cells* (Wiley, Hoboken, NJ, 2015), Chap. 1, pp. 1–20.
- [10] I. Sychugov, Analytical description of a luminescent solar concentrator, *Optica* **6**, 1046 (2019).
- [11] I. Sychugov, Geometry effects on luminescence solar concentrator efficiency: Analytical treatment, *Appl. Opt.* **59**, 5715 (2020).
- [12] D. S. Wiersma, The physics and applications of random lasers, *Nat. Phys.* **4**, 359 (2008).
- [13] N. B. Nelson and B. B. Prévelin, Calibration of an integrating sphere for determining the absorption coefficient of scattering suspensions, *Appl. Opt.* **32**, 6710 (1993).
- [14] Y. Villanueva, C. Veenstra, and W. Steenbergen, Measuring absorption coefficient of scattering liquids using a tube inside an integrating sphere, *Appl. Opt.* **55**, 3030 (2016).
- [15] J.-C. Ravey and P. Mazon, Light scattering in the physical optics approximation; application to large spheroids, *J. Opt.* **13**, 273 (1982).
- [16] D. Q. Chowdhury, P. W. Barber, and S. C. Hill, Energy-density distribution inside large nonabsorbing spheres by using Mie theory and geometrical optics, *Appl. Opt.* **31**, 3518 (1992).
- [17] A. Macke, Scattering of light by polyhedral ice crystals, *Appl. Opt.* **32**, 2780 (1993).
- [18] L. Bi and P. Yang, Physical-geometric optics hybrid methods for computing the scattering and absorption properties of ice

- crystals and dust aerosols, in *Light Scattering Reviews 8* (Springer, Berlin, 2013), pp. 69–114.
- [19] A. A. Kokhanovsky and E. P. Zege, Local optical parameters of spherical polydispersions: Simple approximations, *Appl. Opt.* **34**, 5513 (1995).
- [20] B. Sun, P. Yang, G. W. Kattawar, and X. Zhang, Physical-geometric optics method for large size faceted particles, *Opt. Express* **25**, 24044 (2017).
- [21] S. A. Ackerman and G. L. Stephens, The absorption of solar radiation by cloud droplets: An application of anomalous diffraction theory, *J. Atmos. Sci.* **44**, 1574 (1987).
- [22] D. L. Mitchell, Parameterization of the Mie extinction and absorption coefficients for water clouds, *J. Atmos. Sci.* **57**, 1311 (2000).
- [23] M. Xu, M. Lax, and R. R. Alfano, Anomalous diffraction of light with geometrical path statistics of rays and a Gaussian ray approximation, *Opt. Lett.* **28**, 179 (2003).
- [24] H. C. van de Hulst, *Light Scattering by Small Particles* (Dover, New York, 1981).
- [25] C. F. Bohren and D. R. Huffman, *Absorption and Scattering of Light by Small Particles* (Wiley, Hoboken, NJ, 2008).
- [26] A. A. Kokhanovsky and A. Macke, Integral light-scattering and absorption characteristics of large, nonspherical particles, *Appl. Opt.* **36**, 8785 (1997).
- [27] W. Gille, The small-angle scattering correlation function of the cuboid, *J. Appl. Crystallogr.* **32**, 1100 (1999).
- [28] R. Savo, R. Pierrat, U. Najar, R. Carminati, S. Rotter, and S. Gigan, Observation of mean path length invariance in light-scattering media, *Science* **358**, 765 (2017).
- [29] F. Tommasi, L. Fini, F. Martelli, and S. Cavalieri, Invariance property in inhomogeneous scattering media with refractive-index mismatch, *Phys. Rev. A* **102**, 043501 (2020).
- [30] E. Yablonovitch, Statistical ray optics, *J. Opt. Soc. Am.* **72**, 899 (1982).
- [31] See Supplemental Material at <http://link.aps.org/supplemental/10.1103/PhysRevA.103.L031502> for additional technical details.
- [32] S. Q. Duntley, The optical properties of diffusing materials, *J. Opt. Soc. Am.* **32**, 61 (1942).
- [33] M. V. Berry, Regularity and chaos in classical mechanics, illustrated by three deformations of a circular ‘billiard,’ *Eur. J. Phys.* **2**, 91 (1981).